# RGC32 promotes the progression of ccRCC by activating the NF-κB/SHP2/EGFR signaling pathway

**Jing Zhang[1,2], Yindi Sun[2], Kai Tang[3], Huirong Xu[4], Junjuan Xiao[1], Yan Li[1]**

[1]Department of Oncology, Shandong Provincial Qianfoshan Hospital, Shandong University, Jinan, China
[2]Department of Oncology, Zibo Central Hospital, Zibo, China
[3]Department of Urology, Zibo Central Hospital, Zibo, China
[4]College of Traditional Chinese Medicine, Shandong University of Traditional Chinese, Jinan, China

**Correspondence to:** Yan Li; **email:** liyan16766@163.com, https://orcid.org/0000-0001-6021-1641

## ABSTRACT

Background: The role and clinical significance of the response gene to complement 32 (RGC32) in various cancers have been documented, yet its implications in clear cell Renal Cell Carcinoma (ccRCC) remain underexplored.
Methods: This study investigated RGC32's diagnostic and prognostic relevance in ccRCC using bioinformatics methods with data from The Cancer Genome Atlas (TCGA) and the Gene Expression Omnibus (GEO). The impact of RGC32 on ccRCC progression was assessed through nude mouse tumor assays. Immunohistochemistry evaluated RGC32 levels in ccRCC and adjacent normal tissues, while cell proliferation, migration, and invasion capabilities were analyzed using CCK-8, monoclonal proliferation assays, Transwell, and wound healing assays, respectively. Western blotting measured relevant protein expressions.
Results: Bioinformatics analysis highlighted RGC32's significant role in ccRCC pathogenesis. Elevated RGC32 expression in ccRCC tissues was linked to disease progression. Functionally, RGC32 was found to enhance the expression of proteins such as p-PI3K, CyclinA1, CyclinD1, p-STAT3, MMP2, MMP3, MMP9, p-SMAD2/3, Snail, Slug, and N-Cadherin via the NF-κB/SHP2/EGFR pathway, while decreasing E-cadherin levels. Moreover, RGC32 facilitated ccRCC cell proliferation, migration, invasion, and epithelial-mesenchymal transition (EMT).
Conclusion: RGC32 is a pivotal factor in ccRCC development, primarily through the activation of the NF-κB/SHP2/EGFR signaling pathway.

## INTRODUCTION

Renal cell carcinoma constitutes an increasingly prevalent malignancy, characterized by alarming mortality and progressive morbidity rates globally. Among its subtypes, kidney renal clear cell carcinoma (KIRC), also known as ccRCC, represents the predominant form, comprising approximately 70% of all renal cancers [1]. In 2020, global cancer statistics indicated that kidney cancer was the 16th most common cancer in the world, accounting for 2.2% of the total cancer incidence with 431,288 new cases and 1.8% of the total case mortality with 179,368 deaths annually [2]. The insidiousness of ccRCC lies in its propensity for extensive metastasis and subsequent high fatality; nevertheless, prognosis significantly improves with prompt diagnosis and early-stage intervention [3]. Tragically, at the point of clinical diagnosis, an estimated 15% of RCC patients are already burdened with distant metastases, which severely diminishes their survival prospects [4]. Post-curative treatment relapse or metastasis afflicts nearly 30% of patients. The therapeutic challenge with ccRCC is its notorious resistance to conventional radiotherapy and chemo-

**Table 1. The sample information of TCGA and four datasets in gene expression omnibus database.**

| Dataset | Platforms | Normal | Tumor |
|---|---|---|---|
| TCGA | | 72 | 542 |
| GSE15641 | GPL96 (HG-U133A) Affymetrix Human Genome U1334 Array | 23 | 69 |
| GSE40435 | GPL10558 Illumina HumanHT-12 v4.0 expression beadchip | 101 | 101 |
| GSE46699 | GPL570 (HG-U133_Plus_2) Affymetrix Human Genome U133 Plus 2.0 Array | 63 | 67 |
| GSE53757 | GPL570 (HG-U133_Plus_2) Affymetrix Human Genome U133 Plus 2.0 Array | 72 | 72 |

therapy modalities [5]. Consequently, metastatic RCC (mRCC) bears a dismal prognosis, with ten-year survival rates plummeting below 5% [6]. Accordingly, there emerges a critical imperative to discover and validate biomarkers for the efficacious early diagnosis and prognosis of ccRCC, alongside developing targeted therapeutic strategies.

Human Complement response gene 32 (RGC32), positioned at chromosomal locus 13q14.11, spans a genomic length of 1126 base pairs comprising five exons and four introns, and encodes a peptide chain of 137 amino acids. Despite a reduction by 20 amino acid residues at its N-terminus relative to the murine equivalent, human RGC32 shares an impressive 92% congruence with the amino acid sequence of its murine counterpart. As a gene responsive to complement activation, RGC32 is ubiquitously and robustly expressed across diverse normal human tissues, contributing to physiological homeostasis, albeit with noticeable variability in expression levels among different tissues. RGC32 has confirmed expression in liver, kidney, skeletal muscle, placenta, adipose tissues, macrophages, vascular endothelial, and smooth muscle cells. Contrastingly, its expression is markedly lower in brain and heart tissues, and its presence in pulmonary tissues is nearly negligible. The gene plays an instrumental role in the modulation of cell cycle dynamics, immune responses, tumor metastatic processes, and epithelial-mesenchymal transitions. RGC32 has been reported in multiple cancers, including colorectal cancer (CRC), non-small cell lung cancer (NSCLC), breast cancer, cervical cancer, pancreatic cancer, gastric cancer, ovarian cancer and other tumors. It exhibits a characteristic pattern of expression and influence that is both cancer-relevant and tissue-specific. For instance, RGC32 exerts a promotive influence in various tumors such as colorectal, pancreatic, breast, gastric and ovarian cancers, yet inversely affects gliomas and multiple myeloma [7, 8]. Moreover, it displays a bidirectional regulatory effect in non-small cell lung cancer. Despite the extensive research, consensus regarding RGC32's oncogenic role remains elusive, and its specific expression and function in renal clear cell carcinoma are yet undocumented.

Nuclear factor kappa B (NF-κB), a pivotal transcriptional factor, orchestrates a myriad of immune and inflammatory pathways. Existing studies demonstrate a tangible association between RGC32 and NF-κB, where RGC32 is shown to amplify NF-κB's transcriptional activity by directly coupling with the NF-κB subunit p65 and interfacing with the transcription factor's ligand-binding domain, thereby facilitating NF-κB-driven upregulation of effector genes [9].

The present investigation harnesses immuno-histochemical techniques to ascertain RGC32's expression in normal renal and ccRCC tissues, concurrently scrutinizing the correlation between RGC32 expression and ccRCC's clinical parameters, while tentatively probing its role in the ontogenesis and progression of ccRCC.

## MATERIALS AND METHODS

### Publicly-available databases analysis

RNA-seq data and clinical information for ccRCC were obtained from TCGA. We downloaded raw mRNA expression data and SNP data of the renal clear cell carcinoma data for a total of 614 specimens, including the tumor samples ($n = 542$) and the adjacent normal tissues ($n = 72$).

Four sets of microarrays (GSE46699, GSE53757, GSE40435 and GSE15641) were downloaded from the GEO database and used for the validation. Table 1 lists the details of datasets.

According to the expression level of RGC-32, the patients were divided into the high and low expression groups, and the signaling pathway differences between the high and low expression groups were further analyzed by GSEA. Background gene set is the version 7.0 annotated gene set downloaded from MsigDB database as the annotated gene set of subtype pathways, doing differential expression analysis of pathways between subtypes, ranking significantly enriched gene sets (adjusted $p$-value less than 0.05) according to the consistency score.

Clinical data Wax block specimens of 191 renal clear cell carcinoma removed from January 2016 to January 2018 were obtained from the Department of Pathology of Zibo Central Hospital. The privacy rights of human subjects were always observed and with the consent of the patient. Age ranged from 29 to 82, with the median age at 62. Renal clear cell carcinoma according to the 8th edition of AJCC (American Joint Committee on Cancer) renal cancer TNM stage system clinical stage: 108 cases with stage I/II, 70 cases with stage III/IV (The remaining 13 cases could not be staged). Differentiation level: Grade I/II differentiation:65 cases, grade III/IV differentiation: 126 cases, all specimens were confirmed by two senior pathologists, and all specimens were not subjected to anti-tumor therapy such as chemotherapy, radiotherapy and biological therapy. Follow-up immunohistochemical staining experiments were then performed. This study has been approved by the Medical Ethics Expert Committee of Zibo Central Hospital. The approval number is 201805003.

## Cell culture and transfection

HK-2, 786-O and ACHN cell lines were donated by Chao Zhang from the School of Basic Medical Sciences Zhejiang University and cultured in RPMI-1640 medium supplemented with 10% Fetal Bovine Serum (FBS) and 1% penicillin-streptomycin solution. The cells were then placed in a 37°C, 95% air and 5% $O_2$ humidified incubator. 786-O and ACHN cell lines were seeded into 6-well plates ($5 \times 10^4$ cells/well), and transfection was performed using Lipofectamine 2000 after the cells reached 70% confluency. The cells were divided into NC group, RGC32-inhibitor group, NC group, and RGC32-mimic group. After 24 hours of incubation at 37°C with 5% $CO_2$, the 786-O and ACHN cells in NC group and RGC32-inhibitor group were infected with shRNA-SHP2 when the transfection rate reached 80% for subsequent experiments.

## Lentiviral infection

The target DNA gene fragment was subcloned into a lentiviral vector, and a lentiviral vector overexpressing RGC32 and a silencing SHP2 vector were constructed. Identify the RGC32 fragment using a PCR kit (Promega, Madison, WI, USA) according to the manufacturer's instructions, perform a double digestion using EcoRI and BamHI enzymes, and then proceed to DNA sequencing. HEK 293T cells ($2.5 \times 10^\wedge6$) were seeded in Petri dishes. Approximately 1,800 mL of the lentiviral vector packaging system was added to the cells at a density of 60–70%. After collecting the

supernatant, 293T cells are infected with a high concentration of lentivirus.

786-O and ACHN cells from the index growth phase were seeded onto 24-well plates with $10^4$ cells/well. The virus contained supernatant was added to the cells at a density of 70–80%, respectively. After 72 h, the transfection ratio was determined by fluorescence microscopy. More than 80% of cells were successfully transfected.

## Xenograft experiment in nude mice

Twenty-four 6-week-old BALB/c nude mice were purchased from Shanghai Lingchang Biotechnology Co., Ltd. RGC32-OE and its negative control, as well as 786-O and ACHN cells of SHP2-shRNA, are inoculated into mice at a volume of $1 \times 10^7/200$ μl/mouse. During the inoculation process, the needle was inserted from the upper part of the side waist of the mice, ensuring that the distance from the inoculation site was less than the length of the needle to avoid piercing the skin or muscle layer. The inoculation was completed within 1 hour. Nude mice are euthanized with 20% isoflurane, and the pain of nude mice is minimized during the euthanasia process.

## HE staining

Tumor tissue sections were deparaffinized and stained in hematoxylin solution for several minutes. Hematoxylin for 5 min, hydrochloric acid alcohol acidification for 2 s, ammonia anti-blue for 30 s, then rinse in tap water for 1 hour, then briefly rinse in distilled water. After dehydration in alcohol, the sections were stained with eosin solution for 3 minutes, dehydrated in alcohol, cleared in xylene, mounted with neutral gum, and observed under a light microscope.

## Immunohistochemistry staining

After routine deparaffinization and rehydration, antigen retrieval was performed with pH 6.0 sodium citrate buffer for 3 minutes, followed by incubation with primary antibody RGC32 overnight at 4°C. The next day, the sections were washed and incubated with HRP-conjugated secondary antibody, followed by DAB staining, counterstaining with hematoxylin, dehydration, and mounting.

## CCK-8 assay

786-O and ACHN cells were seeded in a 96-well plate at a density of $5 \times 10^5$ cells/well and cultured at 37°C with 5% $CO_2$. CCK-8 solution (C0038, Shanghai Bio-

Technology Company) was added to each well at 0 h, 24 h, 48 h, and 72 h, and the optical density (OD) value of the CCK-8 mixture was measured at 450 nm wavelength for cell viability analysis.

## Clonal proliferation assay

786-O and ACHN cells were seeded in 6-well plates (800 μL/well) and cultured for 24 hours. After replacement with fresh medium containing 10% serum, the cells were cultured for 2 weeks. The medium was then removed, and the cells were fixed, stained, and counted.

## Transwell assay

### Invasion assay
Matrigel was coated on the bottom of the Transwell chambers, and cell suspensions of each experimental group were added to the upper chamber at a density of $5 \times 10^4$ cells/ml. The lower chamber was filled with PRMI 1640 medium containing 15% FBS. After 48 hours of incubation at 37°C, the cells were fixed, stained, and counted.

### Migration assay
The procedure was the same as the invasion assay except for not using Matrigel.

## Wound healing assay

786-O and ACHN cells were seeded at a density of $5 \times 10^5$ cells/ml and grown overnight in a sterilized culture dish. After the cells had completely covered the bottom of the dish, a scratch was made, and the cells were gently washed with PBS, followed by incubation in serum-free medium for 48 hours. The width of the scratch was analyzed using ImageJ software to determine the healing rate.

## Western blotting

The tumor tissues and 786-O and ACHN cells were digested and lysed using RIPA lysis buffer. Protein quantification was performed using the BCA protein quantification kit. The protein samples were loaded, separated by 10% SDS-PAGE, and transferred to a PVDF membrane. The membrane was blocked with 5% non-fat milk and then incubated with primary antibodies (RGC32, p-NF-κB, p-SHP2, t-SHP2, p-EGFR, p-STAT3, MMP2, MMP3, MMP9, CyclinA1, CyclinD1, p-PI3K, p-SMAD2/3, Snail, Slug, N-Cadherin, E-Cadherin, and GAPDH) overnight at 4°C. After washing, the membrane was incubated with secondary antibodies for 2 hours and visualized using ECL reagent.

## Statistical analysis

Data in this study were analyzed using GraphPad 9.0 software and presented as (X ± S). Independent sample *t*-test was used for comparison between two groups, and one-way ANOVA was used for comparison among multiple groups. A *p*-value of less than 0.05 was considered statistically significant.

## RESULTS

First, data from TIMER2.0 and GEPIA revealed that the overexpression of RGC32 was detected in clear cell renal cell carcinoma (ccRCC) which indicated RGC32 was a novel pathogenic and prognostic factor. We analyzed the relationship between RGC32 and clinical symptoms, and RGC32 was significant with Gender, Grade, T, M, N, and Stage stages. We explored the predictive efficacy of RGC32 by the ROC curve. Higher AUC values indicate a better predictive efficacy, The results indicate that the AUC value of RGC32 in the TCGA dataset is: 0.866 (0.8340.899), The AUC value of RGC32 in the GEO dataset is: GSE53757:0.918 (0.8660.970); GSE15641:0.911 (0.856–0.966); GSE40435:0.940 (0.905–0.976); GSE46699:0.891 (0.829–0.954) (Figure 1). It suggests that RGC32 can better predict the disease development.

Then, according to the HPA database, we preliminarily verified that the expression level of RGC32 in the ccRCC tumor tissues was significantly higher than that in the normal tissues. To investigate the clinicopathological features of RGC32 expression and renal clear cell carcinoma, we staged the patients according to their age, sex, the TNM stage of the tumors, histological grade, T stage and IMDC prognosis grade for grouping. Through the analysis, we found that the difference in the positive rate of expression of RGC32 were statistically significant: The TNM I + II was 89.3%, III + IV was 100% ($P = 0.002$), T ($P = 0.004$), IMDC prognosis grade ($P < 0.001$).

The high expression of RGC32 in ccRCC cancer tissues was 83 cases (100%) and in normal tissues in 95 cases (87.96%), and the expression in different tissues was statistically different ($P < 0.05$), and the positive rate of RGC32 expression was statistically significant. See Table 2.

RGC32 presence is markedly more prevalent in clear cell renal cell carcinoma (ccRCC) compared to normal kidney tissues, with a significant difference ($P < 0.001$). Western blot analysis further confirms that RGC32 levels in ccRCC are considerably higher when

contrasted with adjacent non-cancerous tissues. This pattern of overexpression extends to HK-2, 786-O, and ACHN cell lines, with notably higher levels in the latter two compared to HK-2 cells (Figure 2).

We did this by inoculating 786-O cells and ACHN cells in the NC group and the RGC32-inhibitor group in BALB/c nude mice, respectively. The results showed that the tumor volume and area in the RGC32-OE group
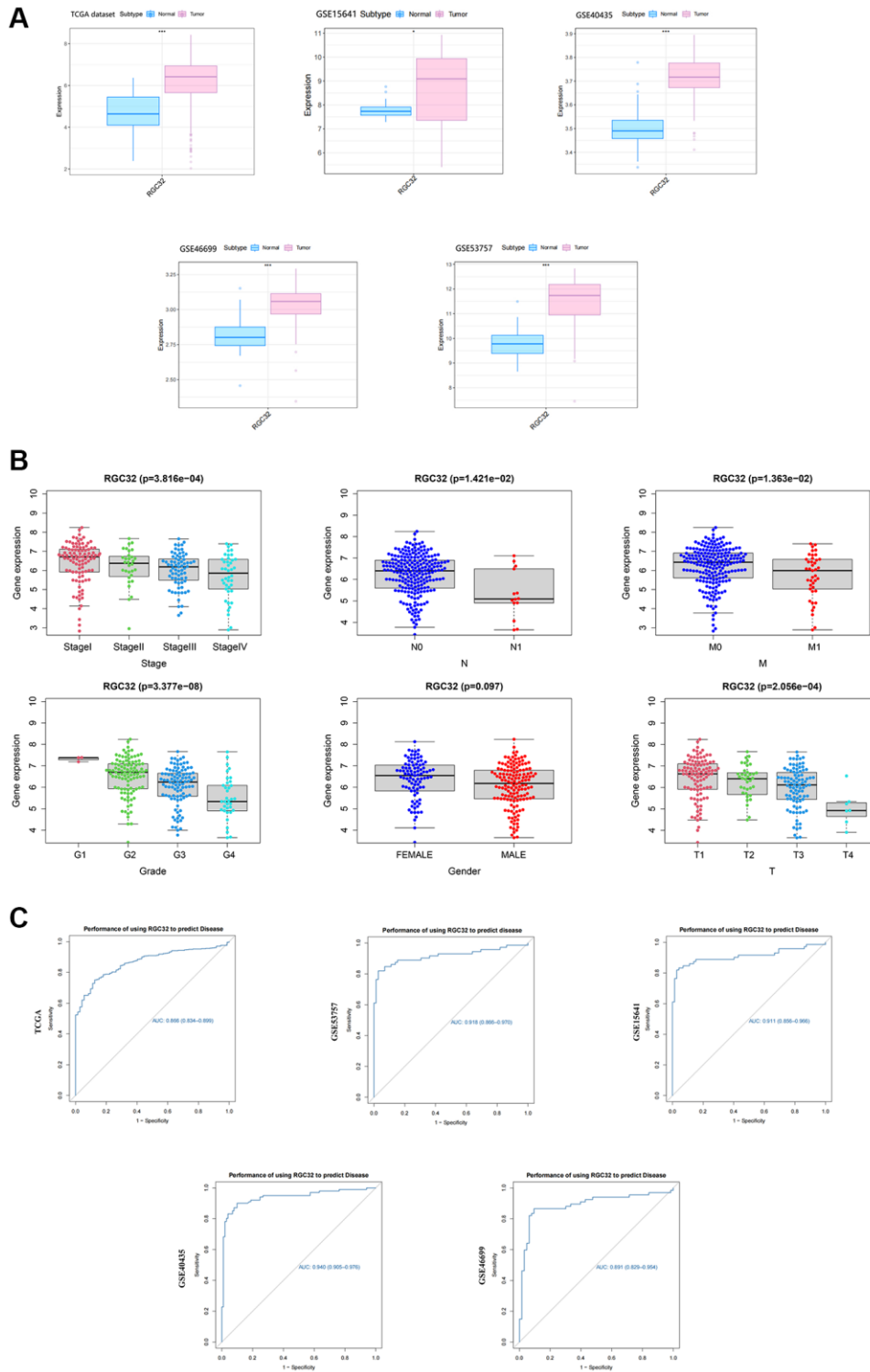


**Figure 1. RGC32 is overexpressed in ccRCC and correlated with clinicopathological features.** (**A**) Data from TIMER2.0 and GEPIA revealed that the overexpression of RGC32 was detected in ccRCC; (**B**) We analyzed the relationship between RGC32 and clinical symptoms, and RGC32 was significant with Gender, Grade, T, M, N, and Stage stages; (**C**) We explored the predictive efficacy of RGC32 by the ROC curve.

**Table 2. Differential expression of RGC32 in adjacent tissues and tumor tissues.**

| | | Normal kidney tissue | | Total | $\chi^2$ | $P$ |
| --- | --- | --- | --- | --- | --- | --- |
| | | Positive | Negative | | | |
| **ccRCC** | **Positive** | 83 (100%) | 95 (87.96%) | 178 | | |
| | **Negative** | 0 (0%) | 13 (12.04%) | 13 | 95 | <0.001 |
| 总计 | | 83 | 108 | 191 | | |
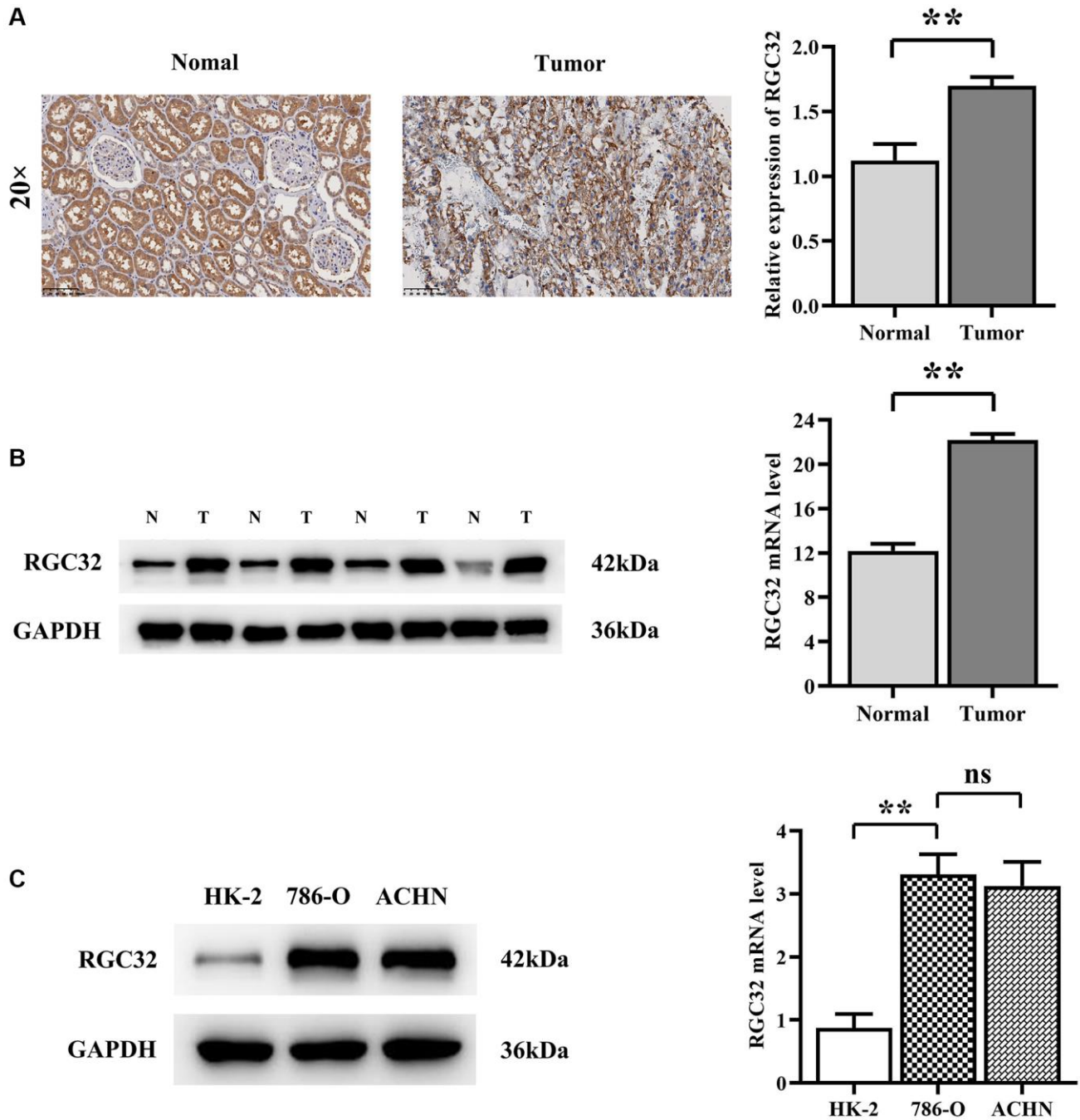


**Figure 2. RGC32 protein expression in ccRCC and normal kidney tissue.** (**A**) Immunohistochemical staining results of ccRCC tissues and normal renal tissues and RGC32 expression statistics; (**B**) Western blotting results of ccRCC tissues and normal kidney tissues, as well as RGC32 expression statistics; (**C**) Western blotting results of HK-2 cells, 786-O cells and ACHN cells and expression statistics of RGC32. $^{**}p <$ 0.01; $^{ns}p > 0.05$.

were significantly increased compared to the NC group. This trend reverses upon SHP2 knockdown, where tumor volume and area decrease significantly, erasing the disparity between groups (Figure 3).

Then, the results of western blotting showed that the protein expressions of RGC32, p-NF-κB, p-SHP2, t-SHP2 and p-EGFR in the RGC32-OE group were significantly increased compared with the NC group. However, after the specific knockdown of SHP2, the expressions of RGC32 and p-NF-κB in the NC group and RGC32-OE group did not change, and the protein expressions of p-SHP2, t-SHP2 and p-EGFR were significantly reduced and the significant differences were eliminated (Figure 4).
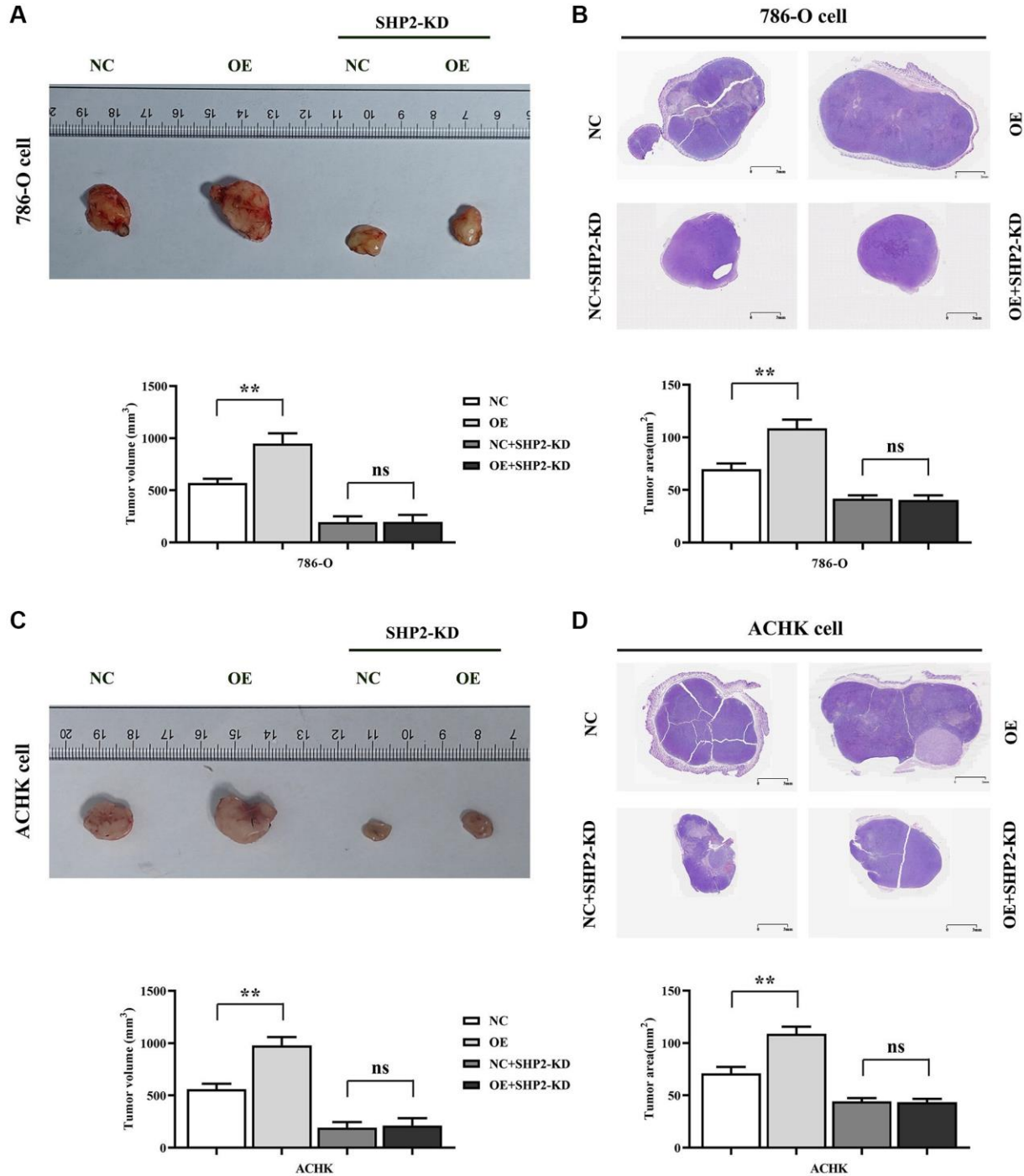


**Figure 3. Specific inhibition of RGC32 can inhibit the progression of ccRCC.** (**A**) Results of tumor-bearing experiments and tumor volume statistics of 786-O cell nude mice; (**B**) The results of HE experiments in 786-O cells and the statistics of tumor slice area; (**C**) Results of tumor-bearing experiments and tumor volume statistics of ACHN cell nude mice; (**D**) The results of HE experiments in ACHN cells and the statistics of tumor slice area. **$p < 0.01$; ns$p > 0.05$.

The results of CCK-8 showed that the OD value of RGC32-mimic group was significantly higher at 72 hours compared with that of NC group. However, after specific knockout of SHP2, the OD value of both the NC group and the RGC32-mimic group was significantly reduced, and the significant difference was eliminated. The results of monoclonal proliferation assay showed that the number of clones in the RGC32-mimic group was significantly higher than that in the NC group. However, after specific knockout of SHP2, the number of clones in both the NC group and the RGC32-mimic group was significantly reduced, and the significant difference was eliminated. The results of western blotting showed that the relative protein expressions of p-PI3K, CyclinA1 and CyclinD1 in the RGC32-mimic group were significantly increased compared with the NC group. However, after the specific knockdown of SHP2, the relative protein expressions of p-PI3K, CyclinA1 and CyclinD1 in the NC group and RGC32-mimic group were significantly reduced and the significant differences were eliminated (Figure 5).

The results of western blotting showed that the relative protein expressions of p-STAT3, MMP2, MMP3 and MMP9 in the RGC32-mimic group were significantly increased compared with the NC group. However, after specific knockdown of SHP2, the relative protein expressions of p-STAT3, MMP2, MMP3 and MMP9 in the NC group and RGC32-mimic group were significantly reduced and the significant differences

were eliminated. The results of wound healing experiment showed that the cell healing rate of the RGC32-mimic group was significantly higher at 48 hours than that of the NC group. However, after specific knockout of SHP2, the cell healing rate at 48 hours was significantly reduced and the significant difference was eliminated in both the NC group and the RGC32-mimic group. The results of Transwell assay showed that the number of migrating and invading cells in the RGC32-mimic group was significantly higher than that in the NC group. However, after specific knockout of SHP2, the number of migrating and invading cells in both the NC group and the RGC32-mimic group was significantly reduced, and the significant difference was eliminated (Figure 6).

Finally, the results of western blotting showed that the relative protein expression of p-SMAD2/3, Snail, Slug and N-cadherin in the RGC32-mimic group was significantly increased and the relative protein expression of E-cadherin was significantly decreased compared with the NC group. However, after specific knockout of SHP2, the relative protein expressions of p-SMAD2/3, Snail, Slug and N-Cadherin in the NC group and RGC32-mimic group were significantly reduced and the significant differences were eliminated. The relative protein expression of E-Cadherin was significantly increased and the significant difference was eliminated (Figure 7). In summation, RGC32 propels ccRCC progression via the NF-κB/SHP2/EGFR signaling axis (Figure 8).
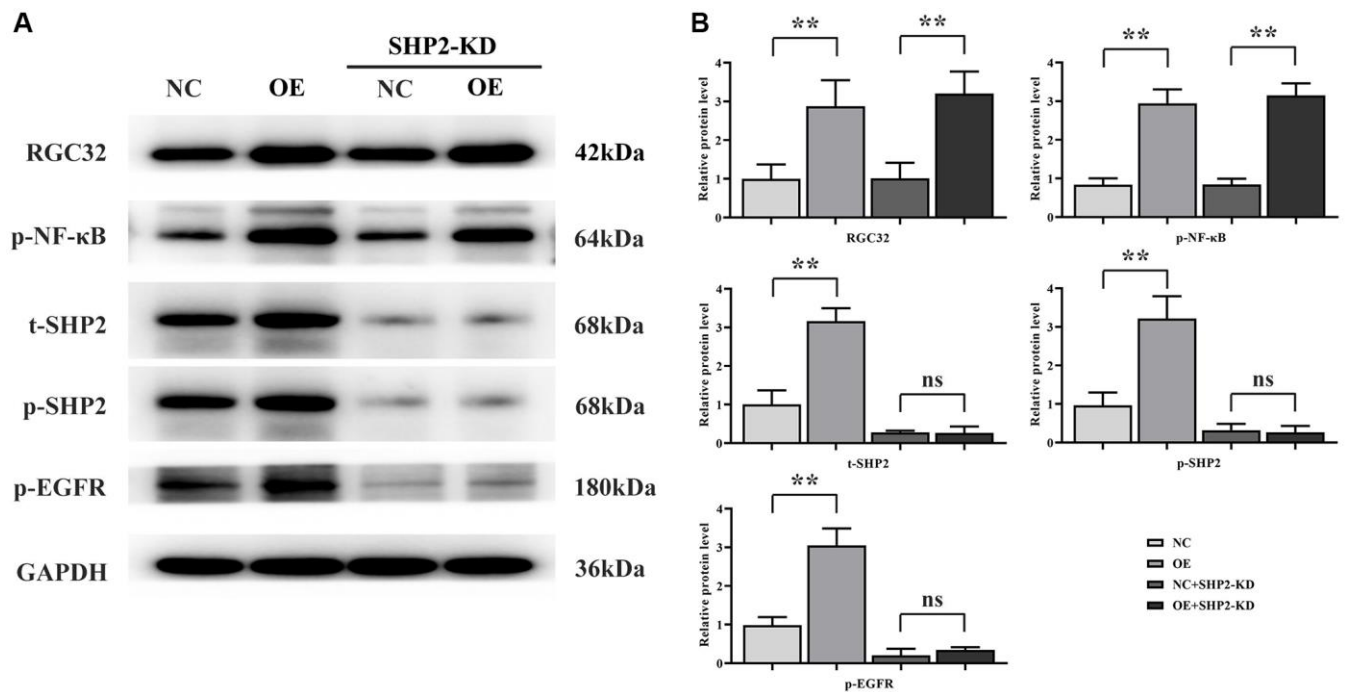


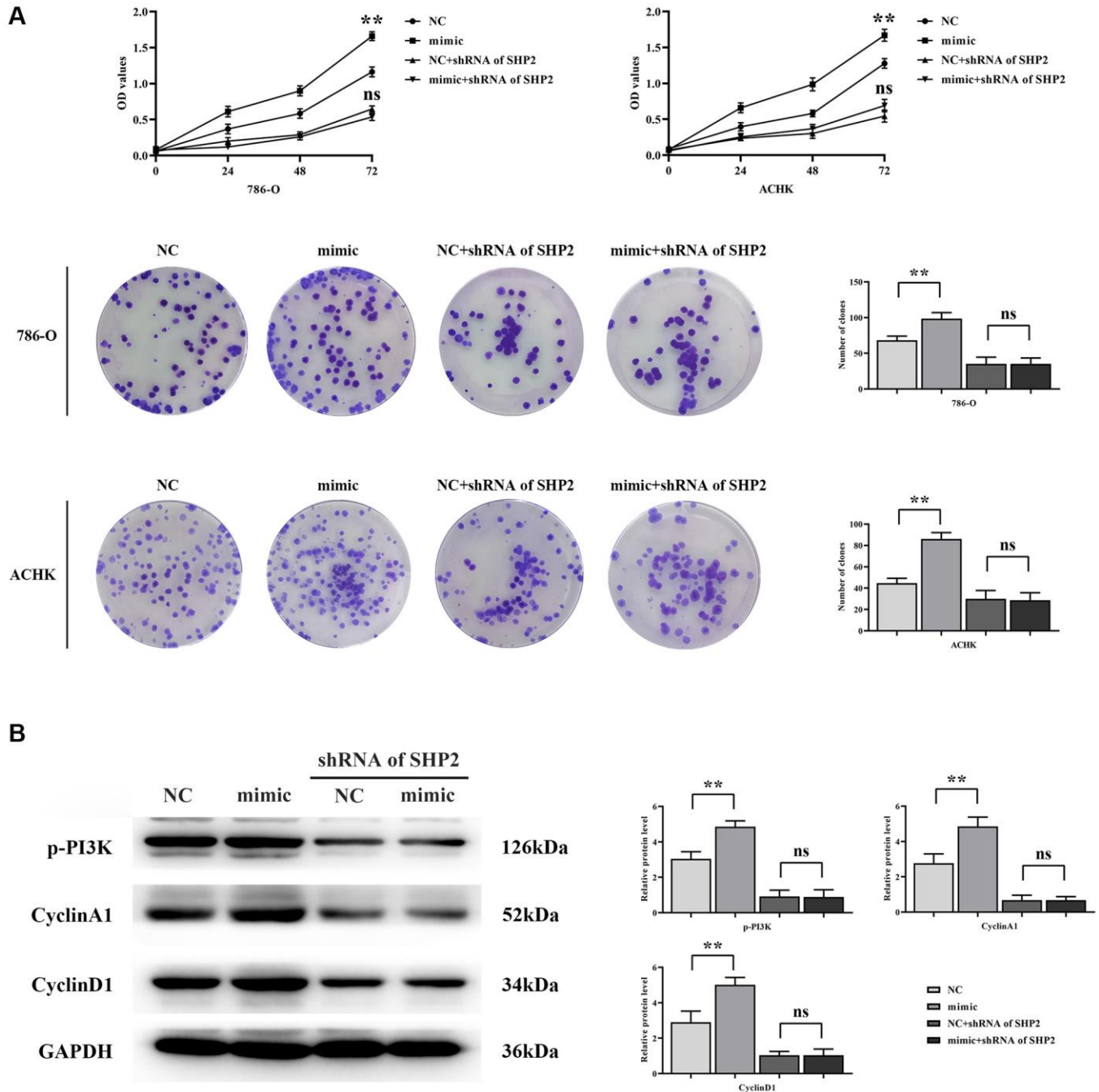**Figure 4. RGC32 can promote phosphorylation of NF-κB, SHP2 and EGFR.** (**A**) Band plots of protein expression for RGC32, p-NF-κB, p-SHP2, t-SHP2 and p-EGFR; (**B**) Relative protein expressions of RGC32, p-NF-κB, p-SHP2, t-SHP2 and p-EGFR. $^{**}p < 0.01$; $^{ns}p > 0.05$.

## DISCUSSION

The RGC-32 gene, first identified in mouse oligodendrocytes by a research collective headed by Horea Rus in 1998, is a gene implicated in the activation of the complement system. The human homolog of RGC-32 is situated at chromosomal location 13q14.11, spans 1,126 base pairs, and comprises 137 amino acids encoded by 5 exons interspersed with 4 introns. Its protein product shares a striking resemblance to those of rat and mouse, exhibiting 92% similarity [10]. Currently, RGC-32 is observed to demonstrate elevated expression levels in the normal cellular matrix of various tissues, namely the placenta, skeletal muscle, kidney, pancreas, liver, and arteries. Conversely, its expression is notably lower in cardiac and cerebral tissues, and mRNA is absent in lung tissues [10–12]. RGC-32 has been implicated as



**Figure 5. RGC32 can mediate the NF-κB/SHP2/EGFR signaling pathway and promote the proliferation of ccRCC cells.** (**A**) CCK-8 and monoclonal proliferation assay results; (**B**) Protein band plots of p-PI3K, CyclinA1 and CyclinD1 and relative protein expression statistics. $^{**}p < 0.01$; $^{ns}p > 0.05$.

playing a pivotal role in the orchestration of the cell cycle, cellular proliferation, differentiation of histiocytes, inflammation mediated by the complement system, cellular repair mechanisms, and the pathophysiology of systemic sclerosis under physiological conditions [13–15]. Recent scholarly scrutiny
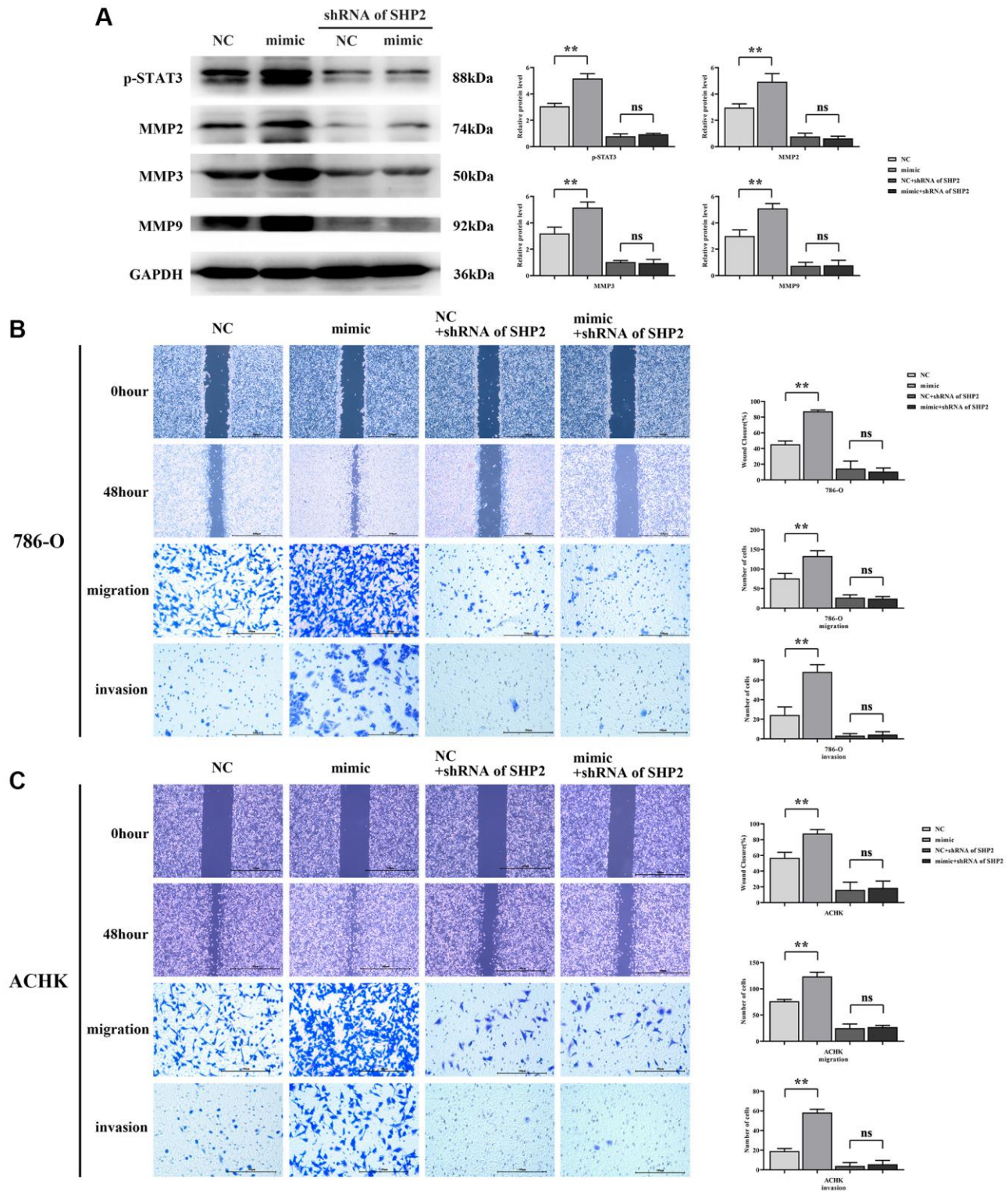


**Figure 6. RGC32 can mediate the NF-κB/SHP2/EGFR signaling pathway and promote the migration and invasion of ccRCC cells.** (**A**) Protein band plots of p-STAT3, MMP2, MMP3 and MMP9 and relative protein expression statistics; (**B**) Wound healing results of 786-O cells at 0 h and 48 h and transwell assay; (**C**) Wound healing results of ACHN cells at 0 h and 48 h and transwell assay. $^{**}p < 0.01$; $^{ns}p > 0.05$.

**Figure 7. RGC32 can mediate the NF-κB/SHP2/EGFR signaling pathway and promote the progression of EMT in ccRCC.** (**A**) Band plots of protein expression for p-SMAD2/3, Snail, Slug, N-Cadherin and E-Cadherin; (**B**) Relative protein expressions of p-SMAD2/3, Snail, Slug, N-Cadherin and E-Cadherin. $^{**}p < 0.01$; $^{ns}p > 0.05$.



**Figure 8. RGC32 promotes the progression of ccRCC by activating the NF-κB/SHP2/EGFR signaling pathway.**

has centered on the ramifications of RGC-32 within oncological contexts. Notably, Wang et al. unveiled that its expression is markedly augmented in colorectal adenocarcinoma samples in comparison to standard colorectal mucosa; this overexpression correlates with diminished patient survival rates [16]. These findings corroborate the significance of RGC-32 in cancer genesis and progression, offering insights with potential therapeutic applications, notably in the context of lung cancer and novel pharmacological innovations. In our investigation, RGC-32 manifested significantly higher expression levels in clear cell renal cell carcinoma (ccRCC) as opposed to adjacent non-cancerous tissue, with this difference bearing statistical significance.

Elevated RGC32 expression has been linked to enhanced proliferation and invasion of colorectal tumor cells, attributed to the activation of the Smad/sip1 signaling axis which facilitates epithelial-mesenchymal transition (EMT) in colorectal cancer cells. Further research by ESKANDARI NASAB et al. detected heightened RGC32 levels in breast cancer specimens, with observations of methylation at the RGC-32 promoter locus. The study titled "Anlotinib Downregulates RGC32 Provoked by Bevacizumab," published in Frontier in Oncology, established that anlotinib can suppress RGC-32 expression, thereby countering bevacizumab resistance; this posits high RGC-32 expression as an independent prognostic factor associated with adverse outcomes in lung adenocarcinoma patients [17–19]. These findings suggest a new diagnostic and therapeutic avenue for patients with bevacizumab resistance.

This study has illuminated that attenuated RGC32 expression can decelerate the progression of ccRCC. RGC32 has been shown to bolster activation of the NF-κB signaling cascade, where it augments phosphorylation and subsequent degradation of IκBα via the activation of IKK, thus facilitating the nuclear translocation and activation of NF-κB. Upon activation, NF-κB engages with the SHP2 gene promoter, modulating SHP2 expression and phosphorylation either directly or indirectly. SHP2 then interacts with EGFR, enhancing its activity by dephosphorylation of specific tyrosine residues (such as Y992, Y1173) through its phosphatase activity, impacting cellular processes like proliferation and survival. EMT, a fundamental cellular process whereby epithelial cells undergo morphological and functional changes to acquire mesenchymal characteristics, is known to exacerbate tumor cell aggressiveness and metastatic potential. In ccRCC, the EMT process potentially fosters a shift from renal tubular epithelial cells towards a mesenchymal-like phenotype that is more migratory and invasive. RGC32 also facilitates proliferation, migration, invasion, and the EMT process in ccRCC cells by modulating the NF-κB/SHP2/EGFR pathway.

## CONCLUSION

In summation, RGC32 propels ccRCC progression via the NF-κB/SHP2/EGFR signaling axis. This study revealed that NF-κB can promote the activation of SHP2 and the mechanism of action between RGC32 and NF-κB/SHP2/EGFR signaling pathways. The effect of RGC32 on the molecular pathophysiology of ccRCC through NF-κB/SHP2/EGFR signaling pathway was verified. It harbors significant potential as both a diagnostic biomarker and as an immunotherapy target for ccRCC. Furthermore, RGC32 holds substantial prognostic and clinicopathological significance for ccRCC. Future studies should aim to substantiate these findings and elucidate the intrinsic mechanisms involved.

## AUTHOR CONTRIBUTIONS

Jing Zhang: Conceptualization, Methodology, Writing - Original Draft, Experiment; Yindi Sun: Data curation, Investigation, Visualization; Kai Tang: Resources, Validation; Huirong Xu: Formal analysis, Software; Junjuan Xiao: Project administration; Yan Li: Supervision, Validation, Writing - Review and Editing.

## CONFLICTS OF INTEREST

The authors declare no conflicts of interest related to this study.

## ETHICAL STATEMENT AND CONSENT

This study has been approved by the Medical Ethics Expert Committee of Zibo Central Hospital. The approval number is 201805003. The privacy rights of human subjects were always observed and with the consent of the patients.

## FUNDING

## REFERENCES

1. Jonasch E, Walker CL, Rathmell WK. Clear cell renal cell carcinoma ontogeny and mechanisms of lethality. Nat Rev Nephrol. 2021; 17:245–61.
https://doi.org/10.1038/s41581-020-00359-2
PMID:33144689

2. Sung H, Ferlay J, Siegel RL, Laversanne M, Soerjomataram I, Jemal A, Bray F. Global Cancer Statistics 2020: GLOBOCAN Estimates of Incidence and Mortality Worldwide for 36 Cancers in 185 Countries. CA Cancer J Clin. 2021; 71:209–49.
https://doi.org/10.3322/caac.21660
PMID:33538338

3. Guida A, Sabbatini R, Gibellini L, De Biasi S, Cossarizza A, Porta C. Finding predictive factors for immunotherapy in metastatic renal-cell carcinoma: What are we looking for? Cancer Treat Rev. 2021; 94:102157.
https://doi.org/10.1016/j.ctrv.2021.102157
PMID:33607461

4. Bray F, Ferlay J, Soerjomataram I, Siegel RL, Torre LA, Jemal A. Global cancer statistics 2018: GLOBOCAN estimates of incidence and mortality worldwide for 36 cancers in 185 countries. CA Cancer J Clin. 2018; 68:394–424.
https://doi.org/10.3322/caac.21492
PMID:30207593

5. Ljungberg B, Albiges L, Abu-Ghanem Y, Bensalah K, Dabestani S, Fernández-Pello S, Giles RH, Hofmann F, Hora M, Kuczyk MA, Kuusk T, Lam TB, Marconi L, et al. European Association of Urology Guidelines on Renal Cell Carcinoma: The 2019 Update. Eur Urol. 2019; 75:799–810.
https://doi.org/10.1016/j.eururo.2019.02.011
PMID:30803729

6. Wu X, Jiang D, Liu H, Lu X, Lv D, Liang L. CD8^{+} T Cell-Based Molecular Classification With Heterogeneous Immunogenomic Landscapes and Clinical Significance of Clear Cell Renal Cell Carcinoma. Front Immunol. 2021; 12:745945.
https://doi.org/10.3389/fimmu.2021.745945
PMID:34970257

7. Brocard M, Khasnis S, Wood CD, Shannon-Lowe C, West MJ. Pumilio directs deadenylation-associated translational repression of the cyclin-dependent kinase 1 activator RGC-32. Nucleic Acids Res. 2018; 46:3707–25.
https://doi.org/10.1093/nar/gky038
PMID:29385536

8. Vlaicu SI, Tatomir A, Anselmo F, Boodhoo D, Chira R, Rus V, Rus H. RGC-32 and diseases: the first 20 years. Immunol Res. 2019; 67:267–79.
https://doi.org/10.1007/s12026-019-09080-0
PMID:31250246

9. Badea TC, Niculescu FI, Soane L, Shin ML, Rus H. Molecular cloning and characterization of RGC-32, a novel gene induced by complement activation in oligodendrocytes. J Biol Chem. 1998; 273:26977–81.
https://doi.org/10.1074/jbc.273.41.26977
PMID:9756947

10. Badea T, Niculescu F, Soane L, Fosbrink M, Sorana H, Rus V, Shin ML, Rus H. RGC-32 increases p34CDC2 kinase activity and entry of aortic smooth muscle cells into S-phase. J Biol Chem. 2002; 277:502–8.
https://doi.org/10.1074/jbc.M109354200
PMID:11687586

11. Vlaicu SI, Cudrici C, Ito T, Fosbrink M, Tegla CA, Rus V, Mircea PA, Rus H. Role of response gene to complement 32 in diseases. Arch Immunol Ther Exp (Warsz). 2008; 56:115–22.
https://doi.org/10.1007/s00005-008-0016-3
PMID:18373239

12. Fosbrink M, Cudrici C, Niculescu F, Badea TC, David S, Shamsuddin A, Shin ML, Rus H. Overexpression of RGC-32 in colon cancer and other tumors. Exp Mol Pathol. 2005; 78:116–22.
https://doi.org/10.1016/j.yexmp.2004.11.001
PMID:15713436

13. Li Z, Xie WB, Escano CS, Asico LD, Xie Q, Jose PA, Chen SY. Response gene to complement 32 is essential for fibroblast activation in renal fibrosis. J Biol Chem. 2011; 286:41323–30.
https://doi.org/10.1074/jbc.M111.259184
PMID:21990365

14. Zhao P, Wang B, Zhang Z, Zhang W, Liu Y. Response gene to complement 32 expression in macrophages augments paracrine stimulation-mediated colon cancer progression. Cell Death Dis. 2019; 10:776.
https://doi.org/10.1038/s41419-019-2006-2
PMID:31601783

15. Sun C, Chen SY. RGC32 Promotes Bleomycin-Induced Systemic Sclerosis in a Murine Disease Model by Modulating Classically Activated Macrophage Function. J Immunol. 2018; 200:2777–85.
https://doi.org/10.4049/jimmunol.1701542
PMID:29507108

16. Wang XY, Li SN, Zhu HF, Hu ZY, Zhong Y, Gu CS, Chen SY, Liu TF, Li ZG. RGC32 induces epithelial-mesenchymal transition by activating the Smad/Sip1 signaling pathway in CRC. Sci Rep. 2017; 7:46078.
https://doi.org/10.1038/srep46078
PMID:28470188

17. Eskandari-Nasab E, Hashemi M, Rafighdoost F. Promoter Methylation and mRNA Expression of Response Gene to Complement 32 in Breast Carcinoma. J Cancer Epidemiol. 2016; 2016:7680523.
https://doi.org/10.1155/2016/7680523
PMID:27118972

18. Xu R, Shang C, Zhao J, Han Y, Liu J, Chen K, Shi W. Knockdown of response gene to complement 32 (RGC32) induces apoptosis and inhibits cell growth, migration, and invasion in human lung cancer cells. Mol Cell Biochem. 2014; 394:109–18.
https://doi.org/10.1007/s11010-014-2086-3
PMID:24833469

19. Yu T, Wang L, Zhao C, Qian B, Yao C, He F, Zhu Y, Cai M, Li M, Zhao D, Zhang J, Wang Y, Qiu W. Sublytic C5b-9 induces proliferation of glomerular mesangial cells via ERK5/MZF1/RGC-32 axis activated by FBXO28-TRAF6 complex. J Cell Mol Med. 2019; 23:5654–71.
https://doi.org/10.1111/jcmm.14473
PMID:31184423